Inferring the properties of Compact Binary Coalescence events

GW Open Data Workshop #6, 2023

Soichiro Morisaki

Source characterization from data

Credit: B. P. Abbott et al., PRL **116**, no.6, 061102 (2016).

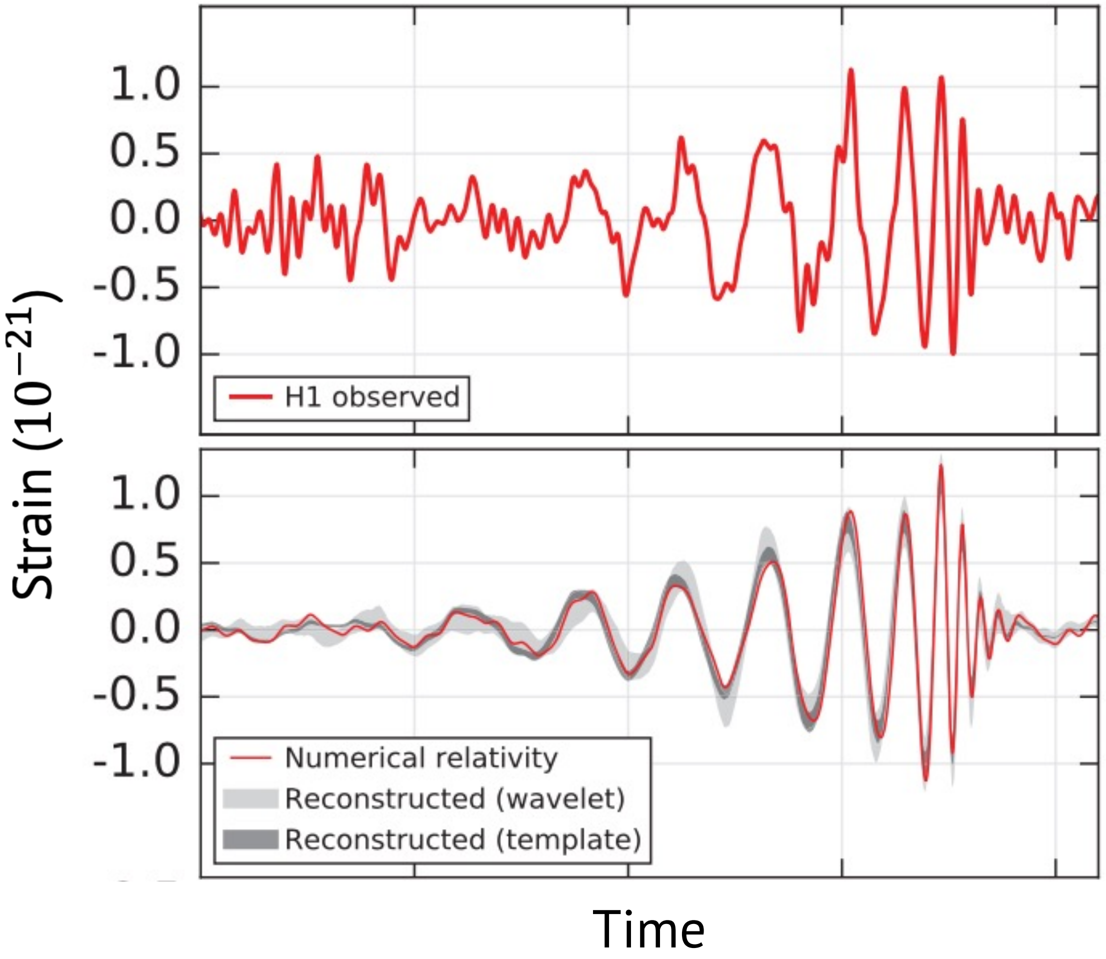

Credit: B. P. Abbott et al., PRL **116**, no.6, 241102 (2016).

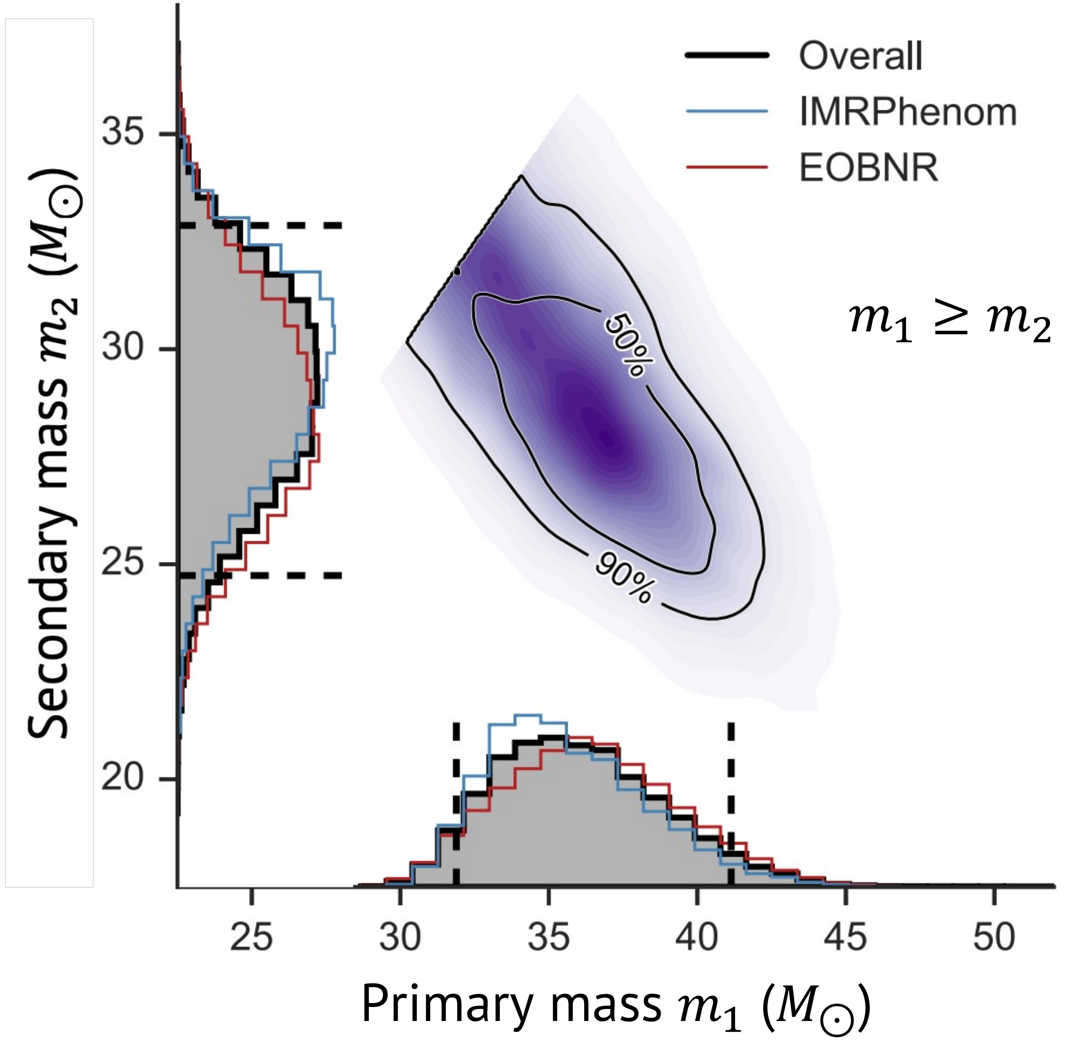

Masses: m_1, m_2

Higher masses

→ Shorter and louder signal

Chirp mass $\mathcal{M}$ is measured most precisely,

$$\mathcal{M} = \frac{(m_1 m_2)^{\frac{3}{5}}}{(m_1 + m_2)^{\frac{1}{5}}}.$$

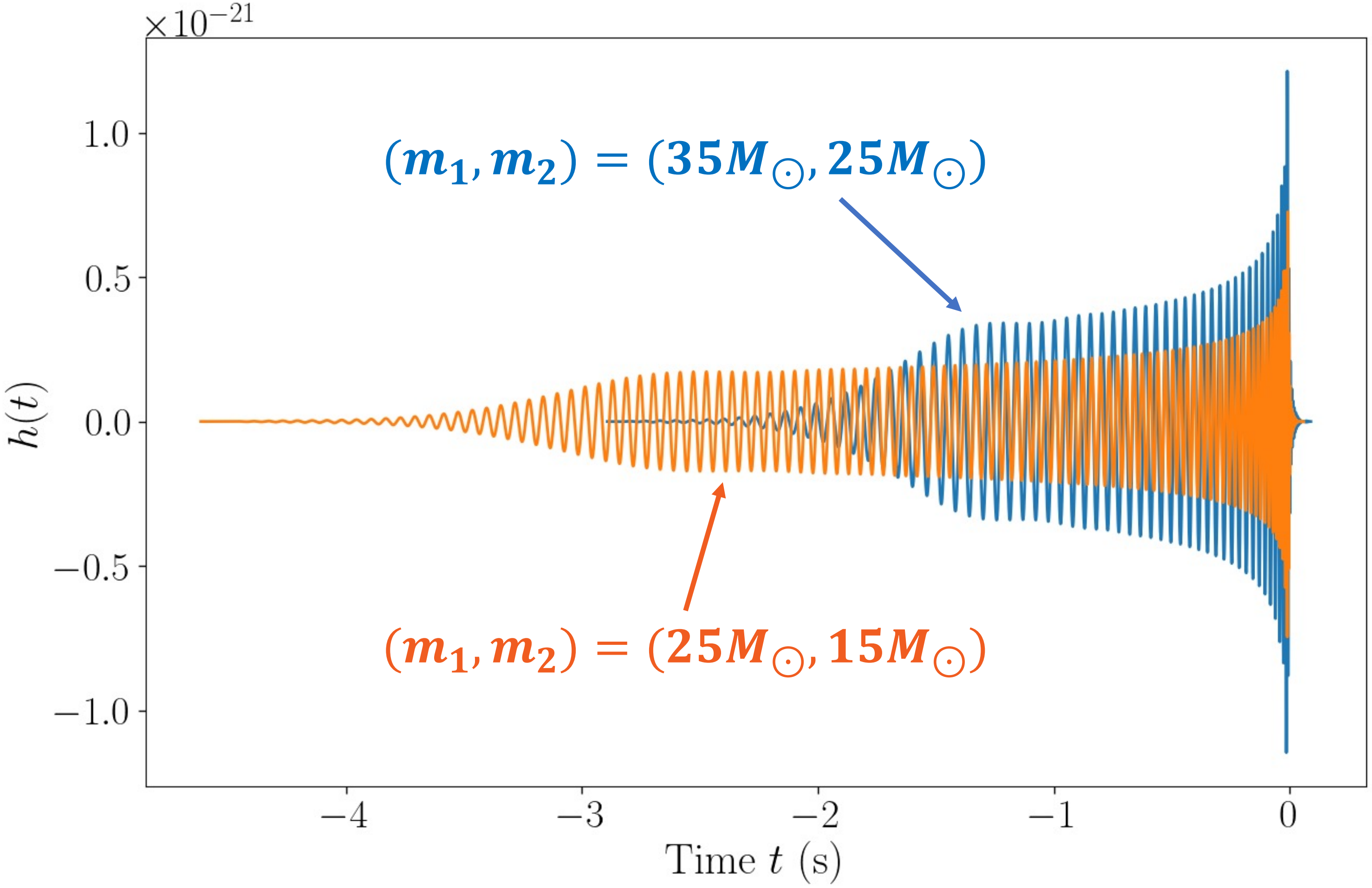

Figure: CBC signal with different masses **starting from 20Hz**

Spins: $\overrightarrow{\chi_1}, \overrightarrow{\chi_2}$

Spins aligned with orbital angular momentum → longer signal

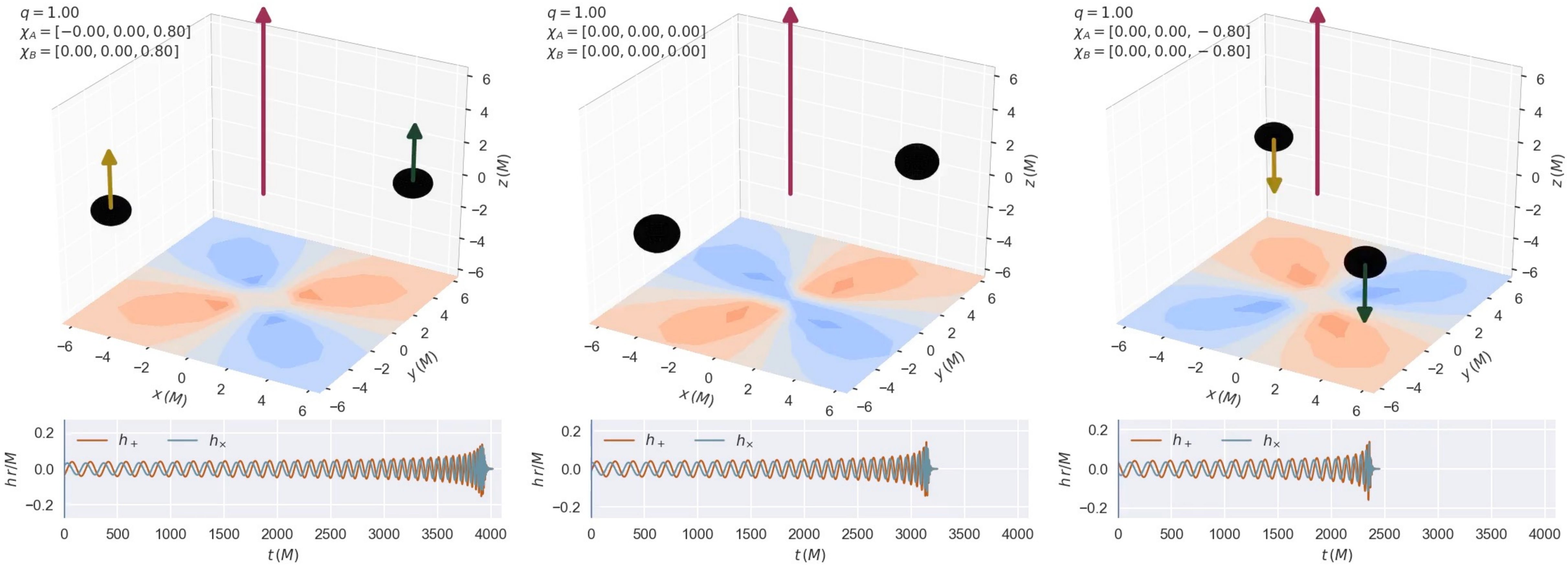

Credit: Vijay Varma et al., Binary Black Hole Explorer

Spins: $\vec{\chi_1}, \vec{\chi_2}$

Orthogonal spin components

→ Precession of orbital plane

→ Amplitude and phase modulation

Masses and spins are key
to probe the formation history of merging binary black holes.

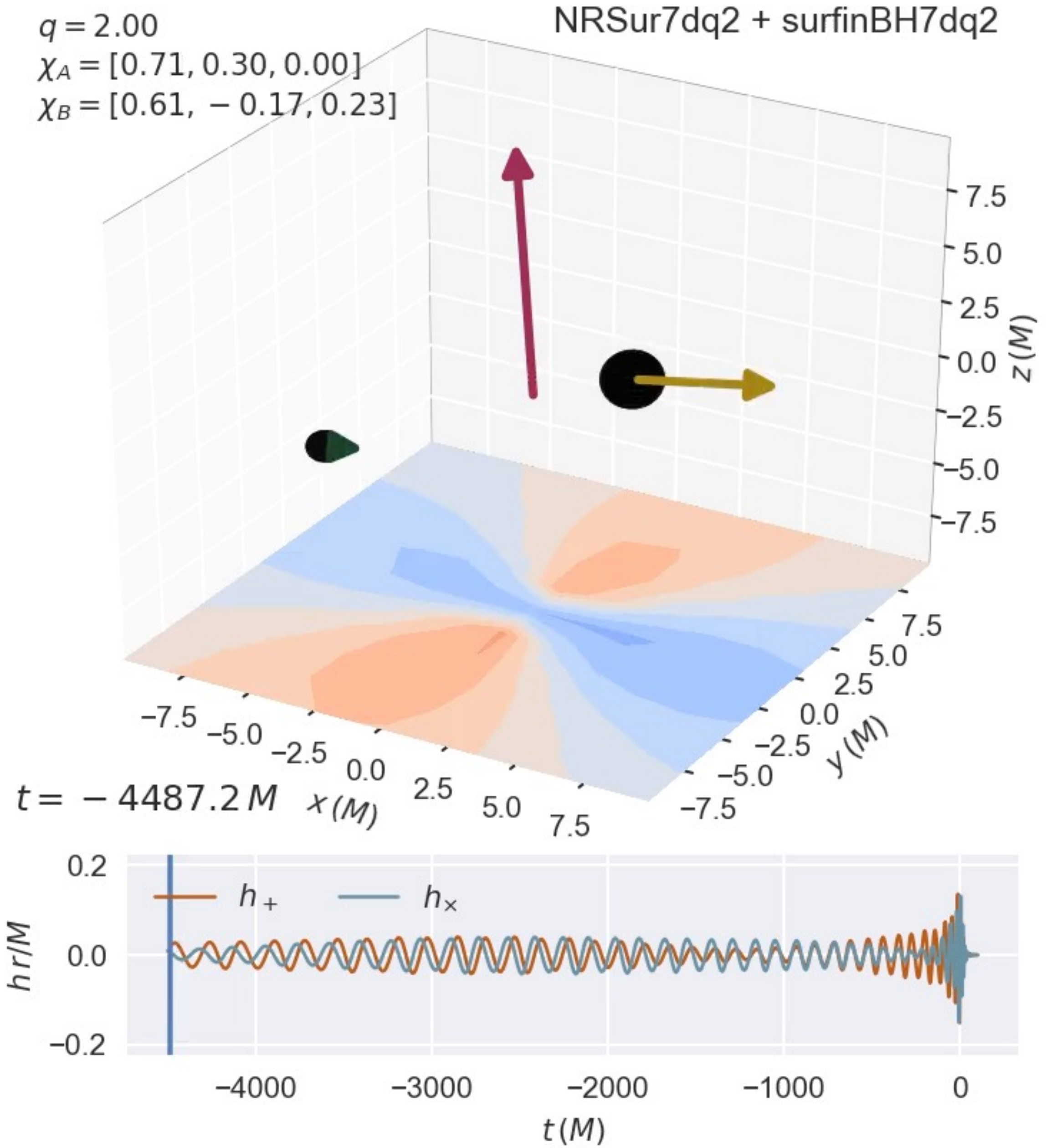

Credit: Vijay Varma et al., Binary Black Hole Explorer

Tidal deformabilities: Λ_1, Λ_2

Tidal deformation of star accelerates orbital motion.

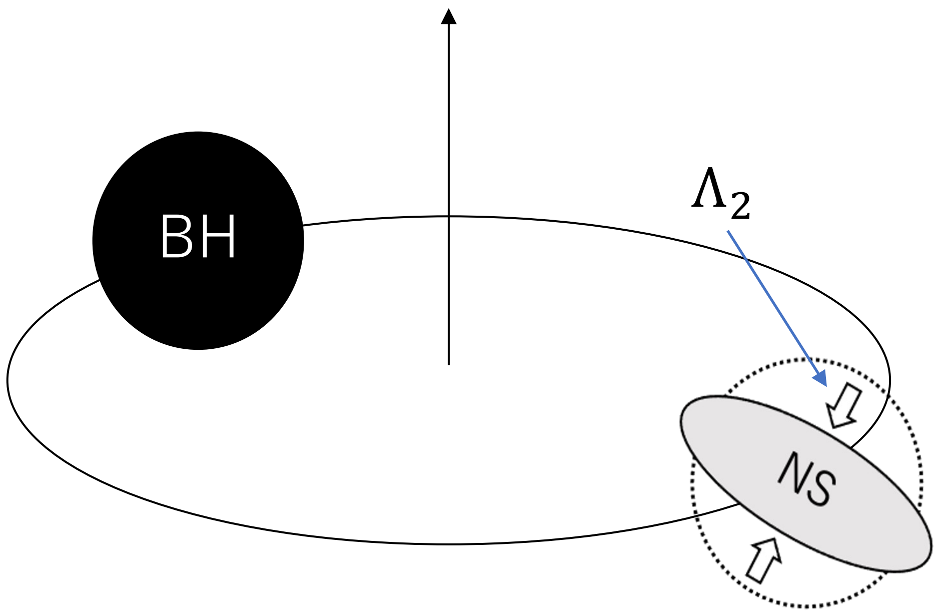

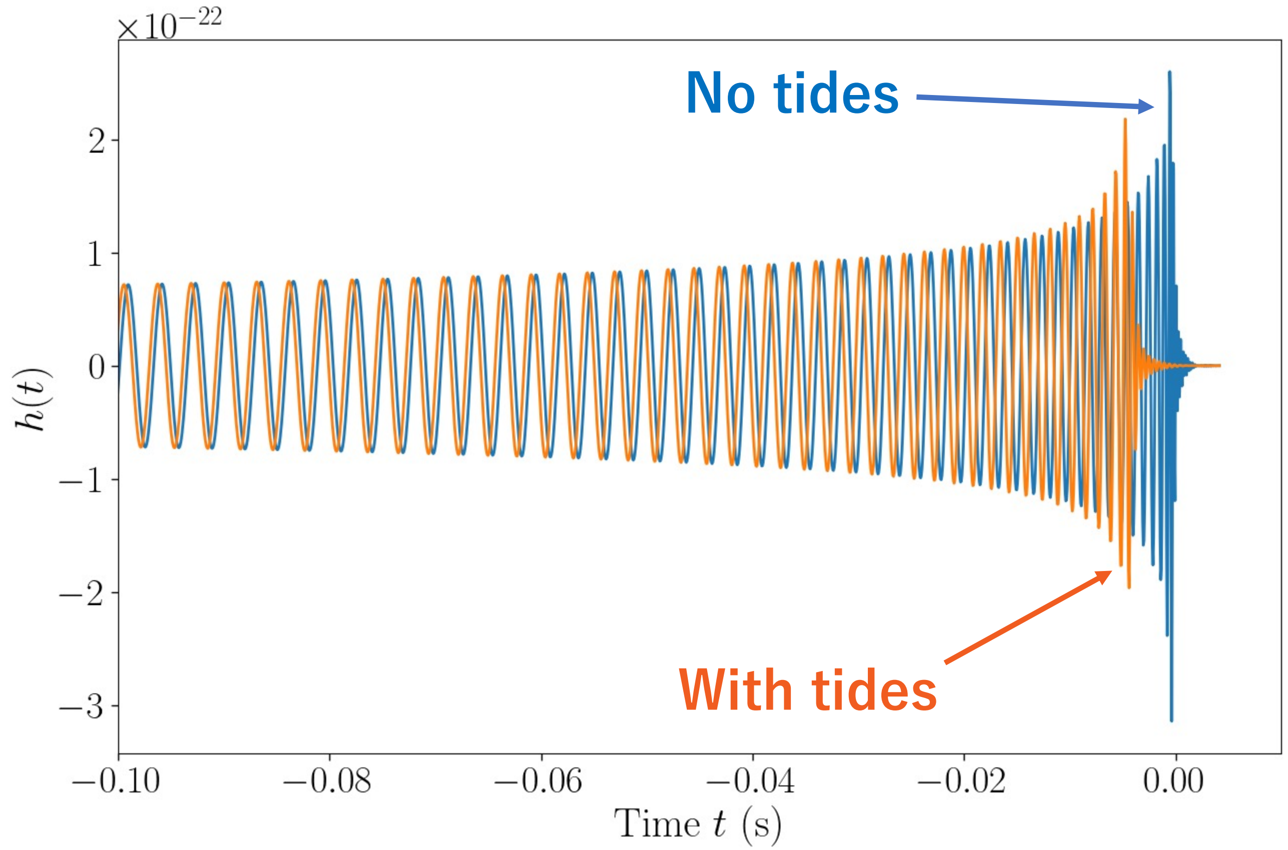

Can constrain the properties of highly dense matter.

Source direction

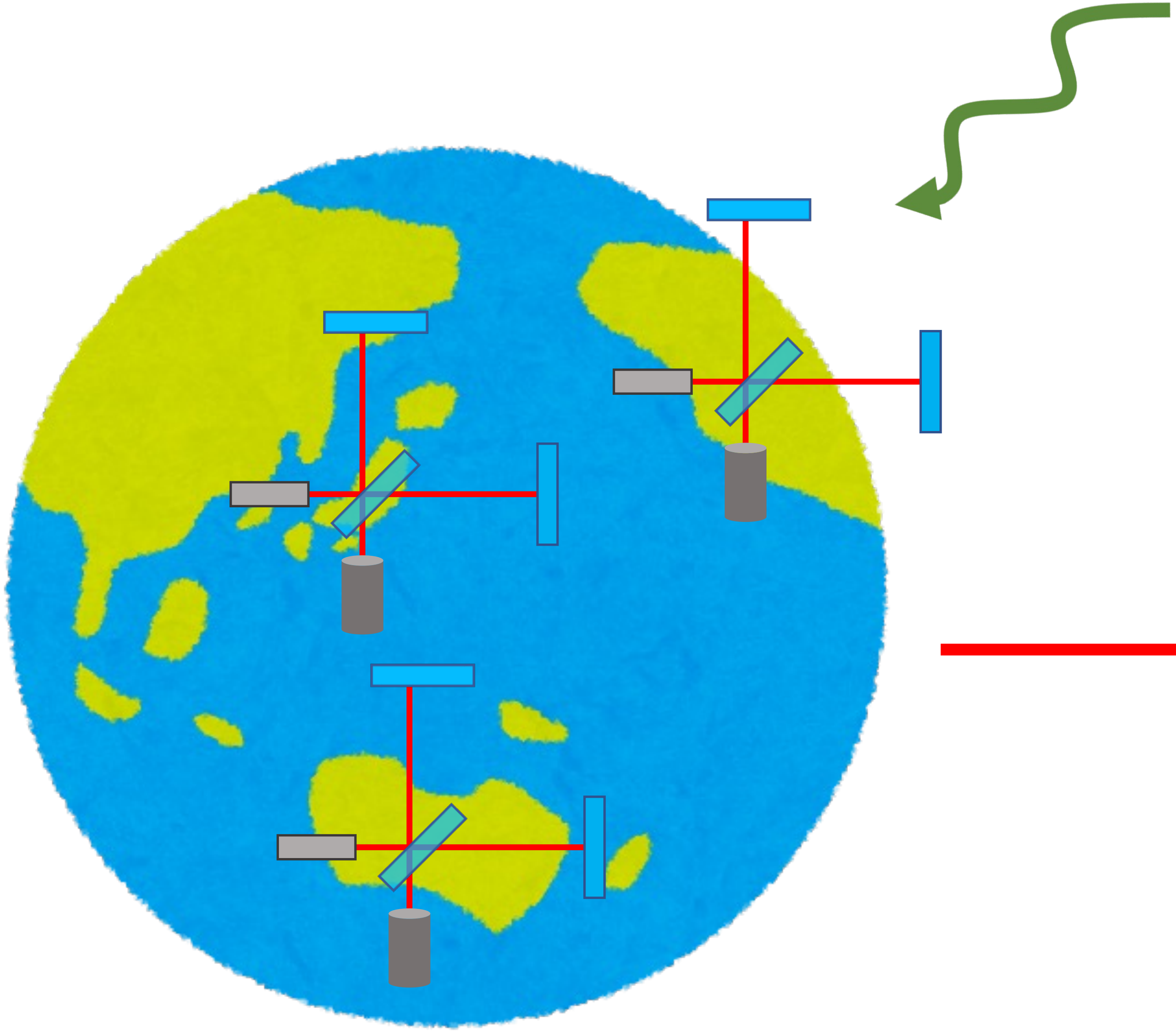

Source direction is estimated with arrival time and signal amplitude observed at multiple detectors.

Credit: B. P. Abbott et al., PRL **116**, no.6, 241102 (2016).

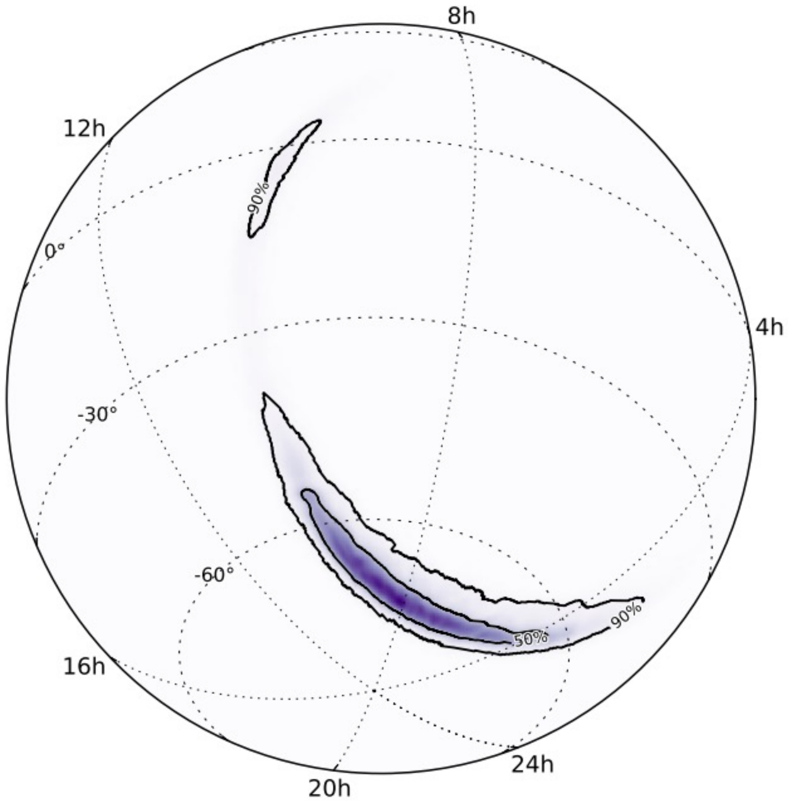

Figure: Estimated source location of GW150914

Source parameters characterizing signal

15 binary black hole parameters + **1** additional parameter **per neutron star**

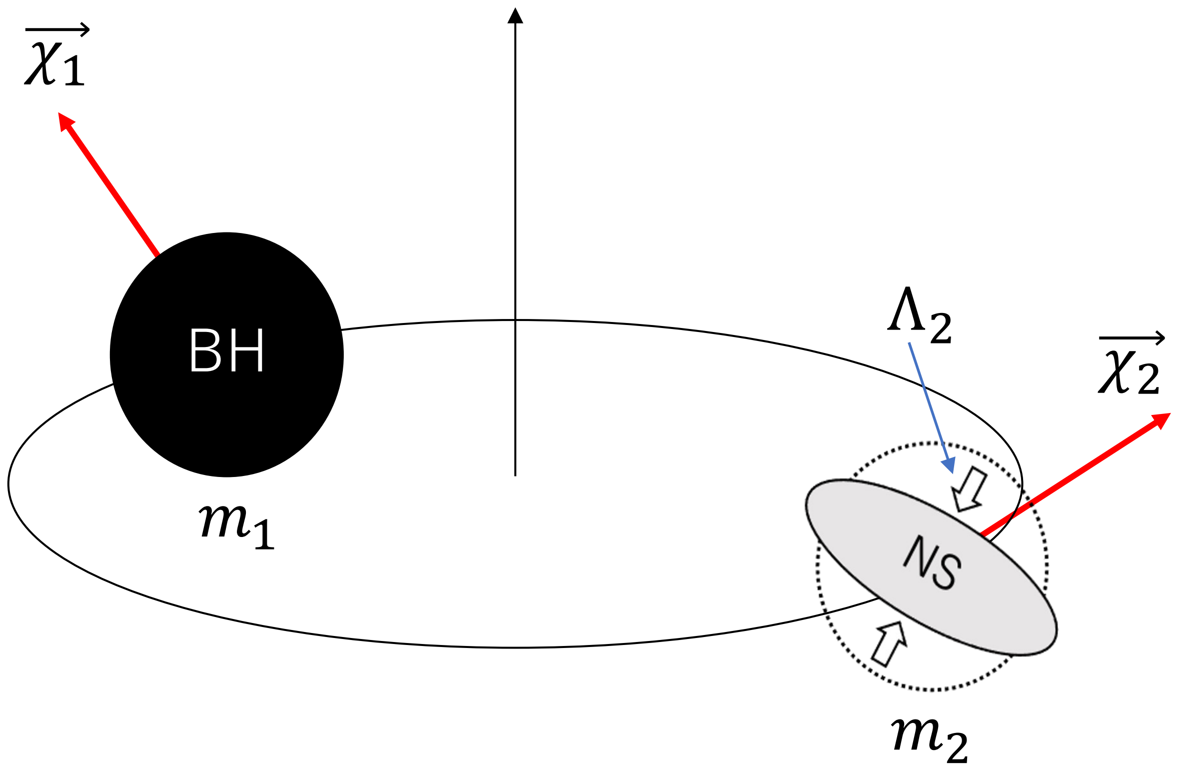

Figure: Schematic picture of neutron star black hole

- Masses: m_1, m_2
  (Chirp mass $\mathcal{M}$ and mass ratio $q \equiv m_2/m_1$ used for efficiency)
- Spins: $\overrightarrow{\chi_1}, \overrightarrow{\chi_2}$
  (Spin magnitudes and angles typically used)
- Tidal deformabilities: Λ_1, Λ_2
  (only for neutron stars)
- Right ascension RA/declination Dec
- Coalescence time t_c
  (Detector frame sky coordinates and time often used for efficiency)
- Luminosity distance D_L
- Orbital inclination angle θ_{JN}
- Polarization angle ψ
- Coalescence phase ϕ_c

Data model

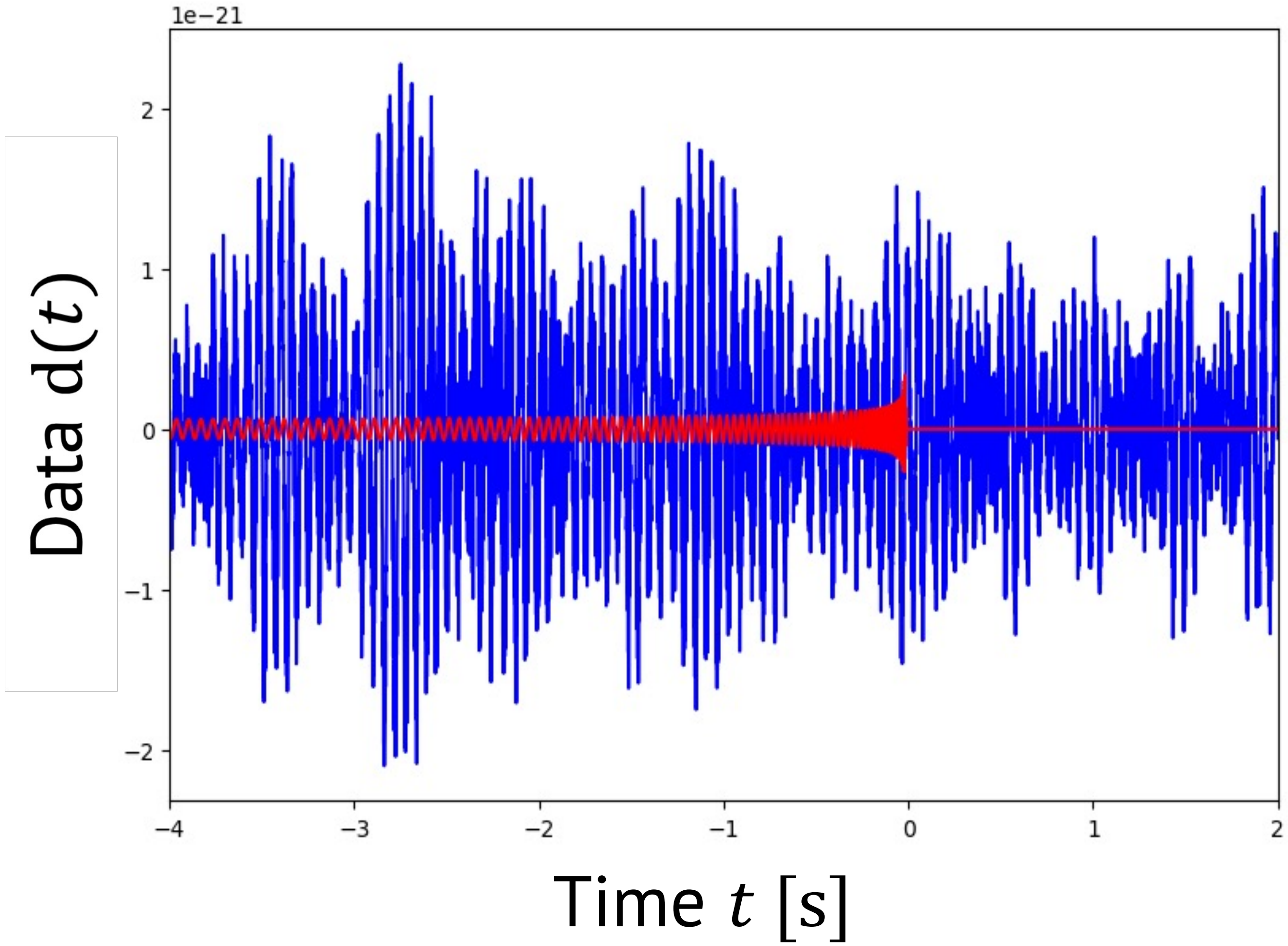

CBC signal Noise

$$d(t) = h(t;\theta) + n(t).$$

θ: parameters
(masses, spins etc.)

Noise model

- Noise is (weakly) stationary: $\langle n(t) \rangle = \mathrm{const.}, \langle n(t)n(t') \rangle = R(|t-t'|)$.

  $\longrightarrow$ $\langle \tilde{n}(f_l) \rangle = 0 \left(f_l = \frac{l}{T} > 0, T\text{: data duration} \right)$, $\langle \tilde{n}^*(f_l)\tilde{n}(f_{l'}) \rangle = \frac{TS(f_l)}{2} \delta_{ll'}$.

  $S(f_l) = \frac{2\langle |\tilde{n}(f_l)|^2 \rangle}{T}$ is referred to as Power Spectral Density (PSD) and characterizes noise variance at f_l.

- Noise follows Gaussian distribution.

Those assumptions lead to Whittle likelihood,

$$p(\tilde{n}(f_l)) = \exp\left(-\frac{2|\tilde{n}(f_l)|^2}{TS(f_l)} \right), \qquad p(\tilde{n}(f_1), \tilde{n}(f_2), \ldots) = \prod_l p(\tilde{n}(f_l)).$$

See J. Veitch et al. (2015): https://arxiv.org/abs/1409.7215 for more context.

Likelihood $p(d|\theta)$

Likelihood is probability of obtaining data d assuming parameter values θ,

$$p(d|\theta) \propto \exp\left[-\frac{2}{T}\sum_l \frac{|\tilde{n}(f_l)|^2}{S(f_l)}\right] = \exp\left[-\frac{2}{T}\sum_l \frac{\left|\tilde{d}(f_l) - \tilde{h}(f_l;\theta)\right|^2}{S(f_l)}\right].$$

Higher likelihood → Smaller residual $\left|\tilde{d}(f_l) - \tilde{h}(f_l;\theta)\right|$

Generalization to data from multiple detectors: $d_1, d_2, \ldots,$

$$p(\{d_I\}_I|\theta) \propto \prod_I \exp\left[-\frac{2}{T}\sum_l \frac{\left|\tilde{d}_I(f_l) - \tilde{h}_I(f_l;\theta)\right|^2}{S_I(f_l)}\right].$$

PSD estimation

- Average tens-hundreds of data sets which do not contain signal:
  $S(f_l) = \frac{2\langle|\tilde{n}(f_l)|^2\rangle}{T}$.

- Fit the spectra of on-source data to mitigate biases from non-stationary noise (See Littenberg and Cornish (2015): https://arxiv.org/abs/1410.3852).

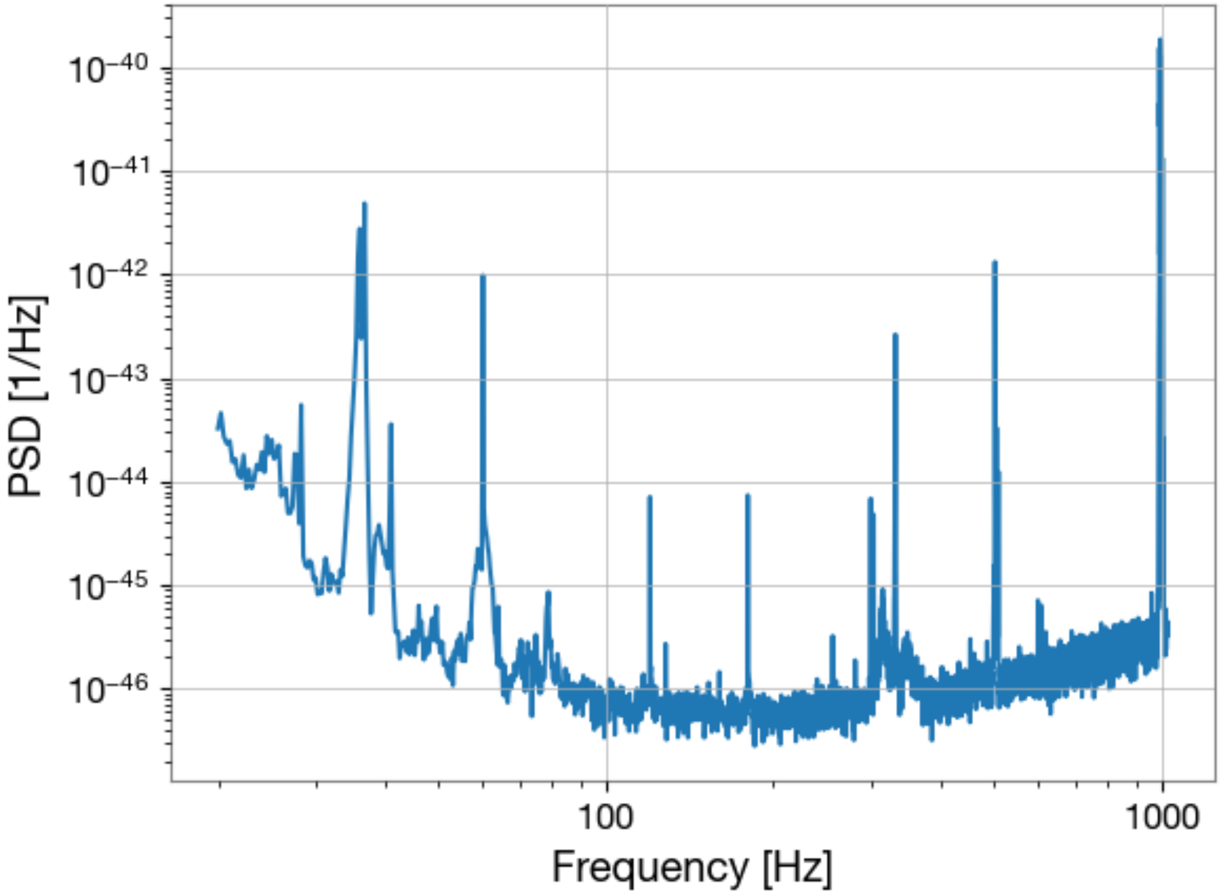

Figure: PSD estimated from data around GW150914

Bayes' theorem

Likelihood ↓ Prior ↓

Posterior → $$p(\theta|d) = \frac{p(d|\theta)p(\theta)}{p(d)}$$ ← Evidence

Bayes' theorem

Likelihood

Prior

Posterior

$$p(\theta|d,M) = \frac{\mathcal{L}(d|\theta,M)\pi(\theta|M)}{\mathcal{Z}(d|M)}$$

Evidence

M: Hypothesis/model

Bayes' theorem

Likelihood   Prior

$$p(\theta|d, M) = \frac{\mathcal{L}(d|\theta, M)\pi(\theta|M)}{\mathcal{Z}(d|M)}$$

Posterior → ; Evidence ←

Prior encodes our prior knowledge or belief on θ.

- No information → Use uninformative prior (e.g. isotropic on RA/Dec, uniform in masses etc.).
- It can incorporate information from electromagnetic observations or astrophysics (e.g. fixed to RA/Dec from electromagnetic obs., astrophysical mass prior etc.).

Bayes' theorem

$$p(\theta|d,M) = \frac{\mathcal{L}(d|\theta,M)\pi(\theta|M)}{\mathcal{Z}(d|M)}$$

Posterior → $p(\theta|d,M)$; Likelihood → $\mathcal{L}(d|\theta,M)$; Prior → $\pi(\theta|M)$; Evidence → $\mathcal{Z}(d|M)$

Evidence can be used for comparing different hypotheses/models (e.g. noise vs signal hypotheses, different waveform models etc.).

$$B = \frac{\mathcal{Z}(d|M_1)}{\mathcal{Z}(d|M_2)}, \qquad B \gg 1 \rightarrow M_1 \text{ is favored}, \qquad B \ll 1 \rightarrow M_2 \text{ is favored}.$$

M_1, M_2: two different hypotheses/models

Curse of dimensionality

- 1D posterior distribution

$$p(m_2|d, M) = \int p(\theta|d, M) \underbrace{dm_1 d\overrightarrow{\chi_1} \mathrm{d}\overrightarrow{\chi_2} \ldots}_{\text{Except for } m_2}$$

- 2D posterior distribution

$$p(\mathrm{RA}, \mathrm{Dec}|d, M) = \int p(\theta|d, M) \underbrace{dm_1 dm_2 d\overrightarrow{\chi_1} \mathrm{d}\overrightarrow{\chi_2}}_{\text{Except for RA, Dec}}$$

They require high-dimensional numerical integration.

Figure credit: R. Abbott *et al.*, ApJL **896** L44 (2020).

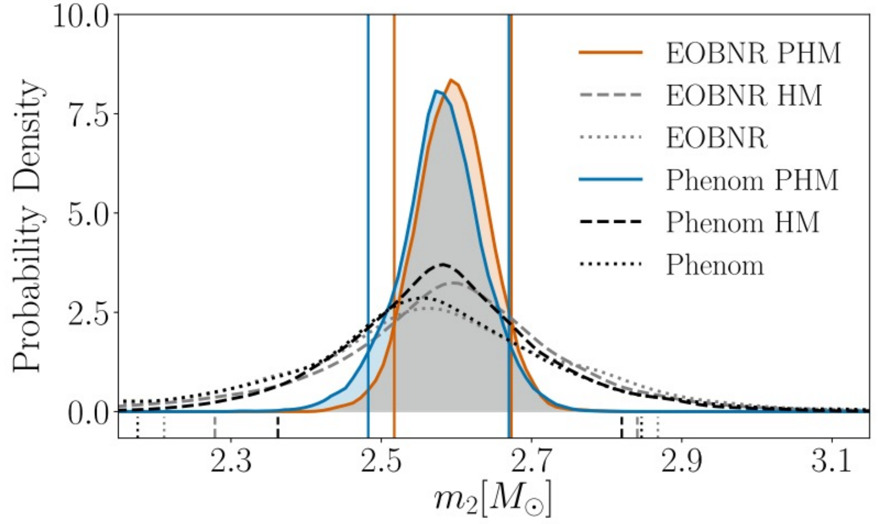

Figure 1: Estimated secondary mass of GW190814

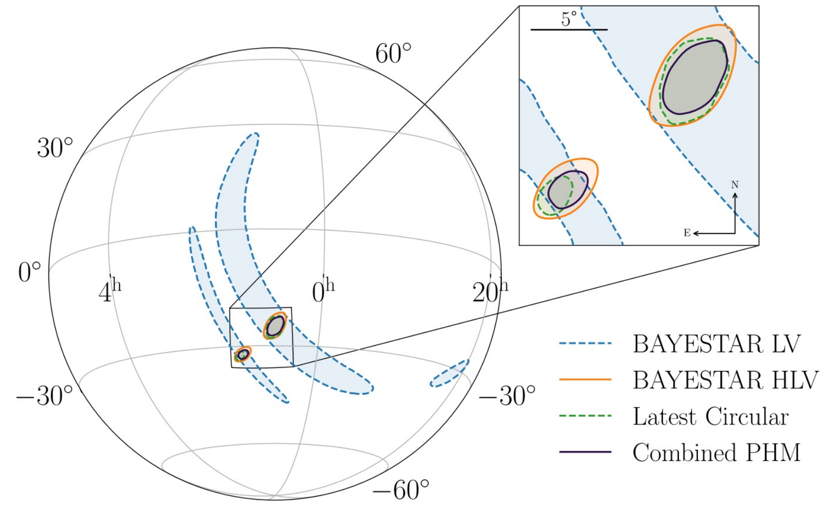

Figure 2: Estimated source location of GW190814

Stochastic sampling

Draw samples from posterior and histogram them!

Various efficient algorithms for sampling
- Markov-chain Monte Carlo (MCMC)
- Nested sampling

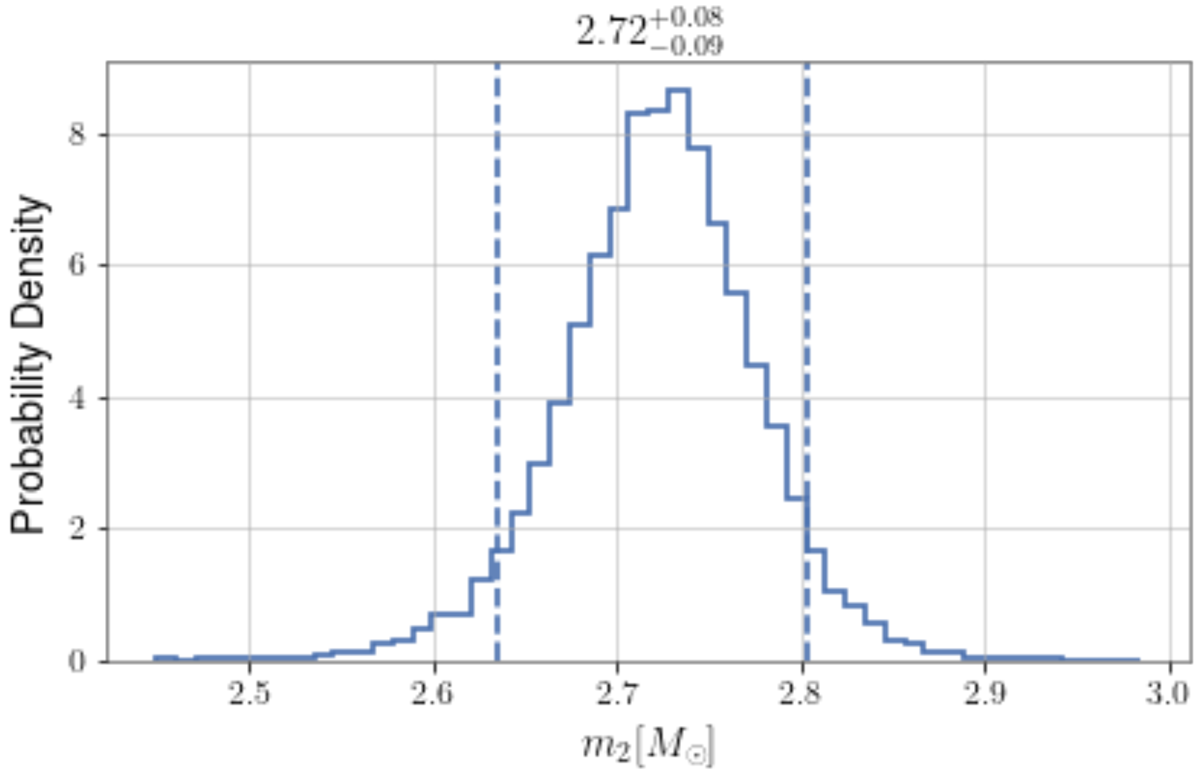

Figure: Estimated secondary mass of GW190814

MCMC example: Metropolis-Hastings algorithm

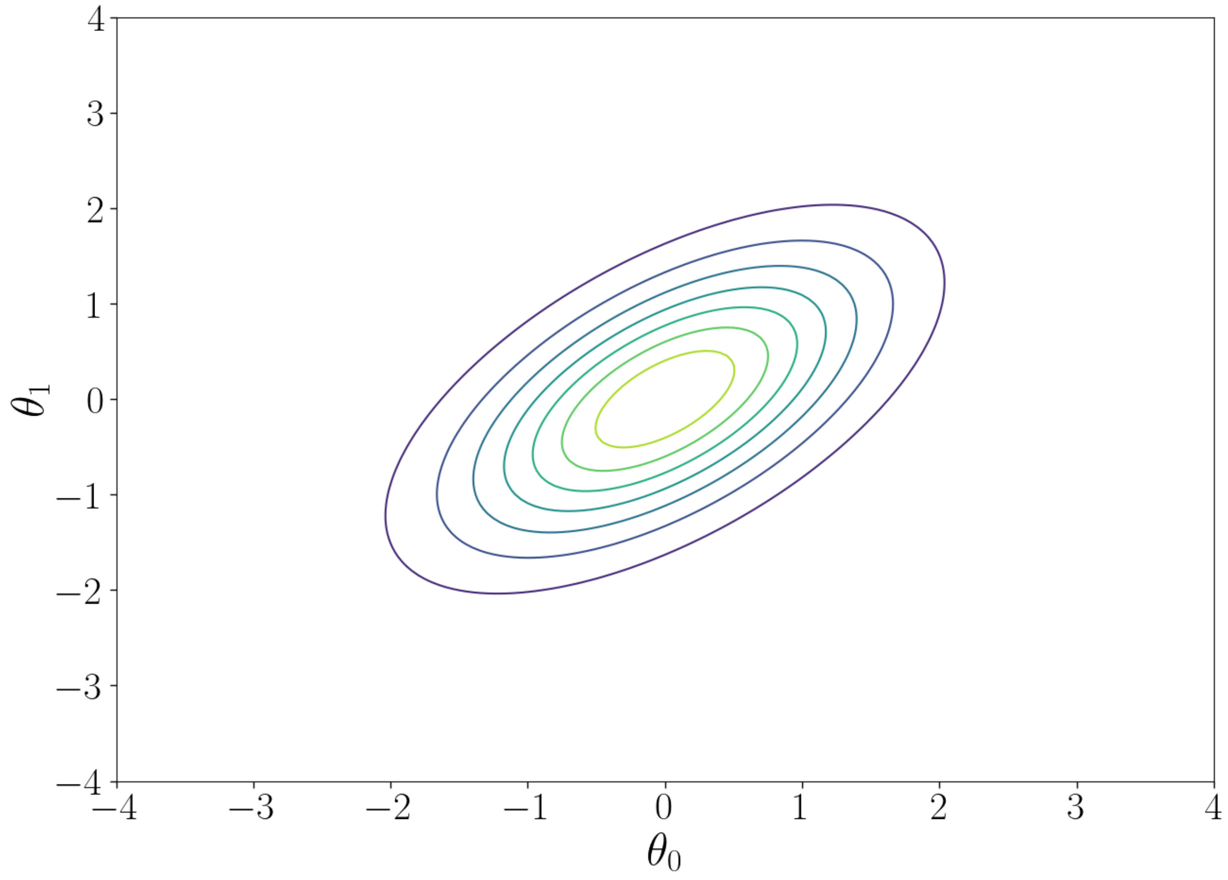

MCMC example: Metropolis-Hastings algorithm

Start from a random point θ.

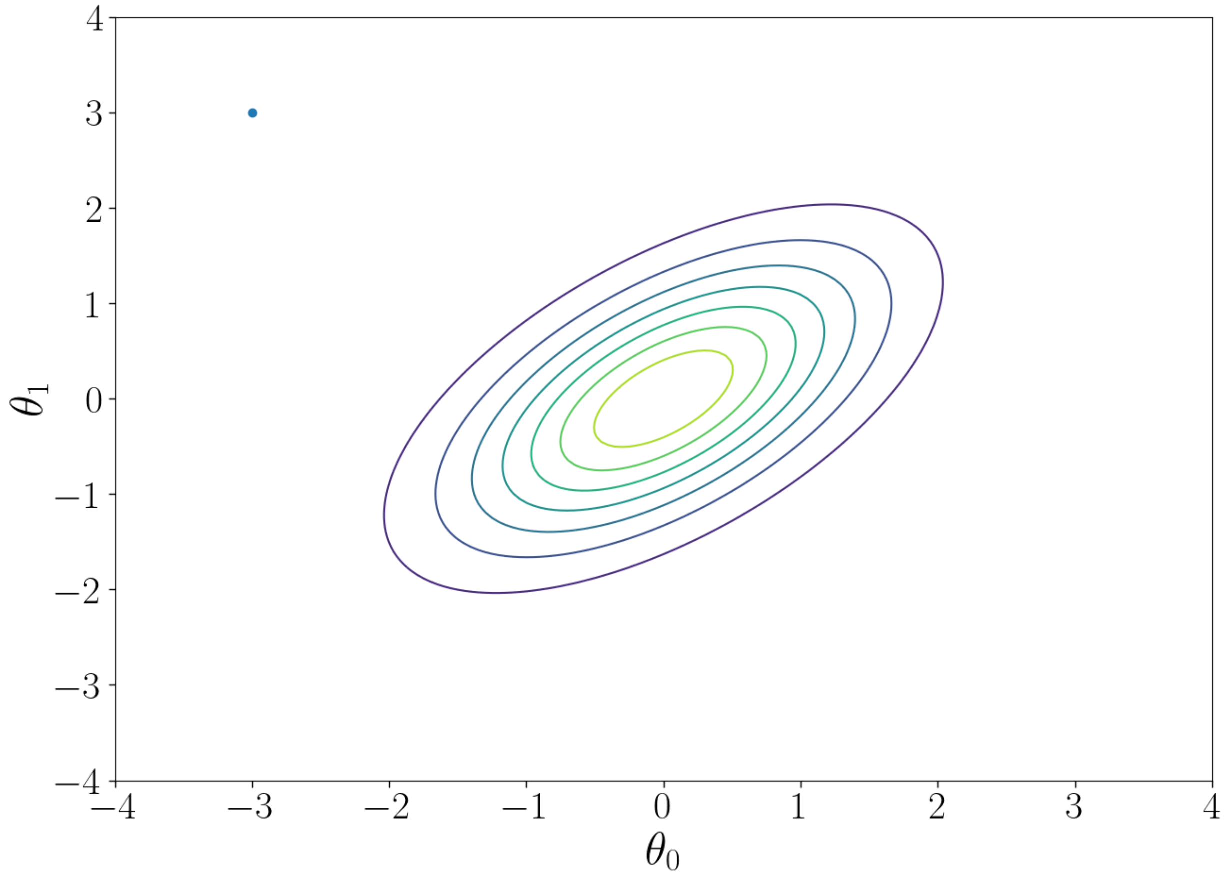

MCMC example: Metropolis-Hastings algorithm

Start from a random point θ.

Propose a next point θ' with proposal distribution $Q(\theta \rightarrow \theta')$. Accept that proposal with probability of $\min\left\{1, \frac{p(\theta'|d,M)Q(\theta' \rightarrow \theta)}{p(\theta|d,M)Q(\theta \rightarrow \theta')}\right\}$.

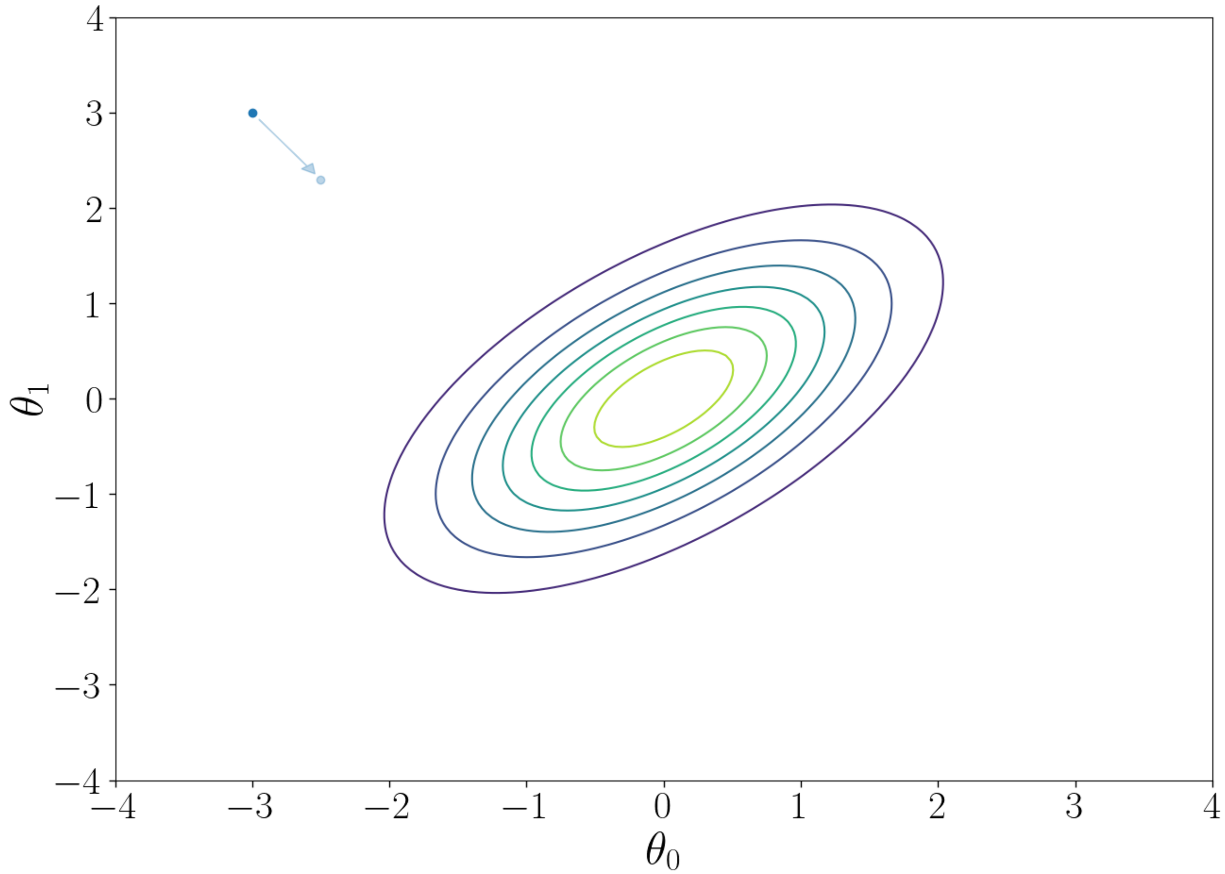

MCMC example: Metropolis-Hastings algorithm

Start from a random point θ.

Propose a next point θ' with proposal distribution $Q(\theta \to \theta')$. Accept that proposal with probability of

$$\min\left\{1, \frac{p(\theta'|d,M)Q(\theta' \to \theta)}{p(\theta|d,M)Q(\theta \to \theta')}\right\}.$$

Repeating this proposal-acceptance, the random point converges to a sample following posterior distribution.

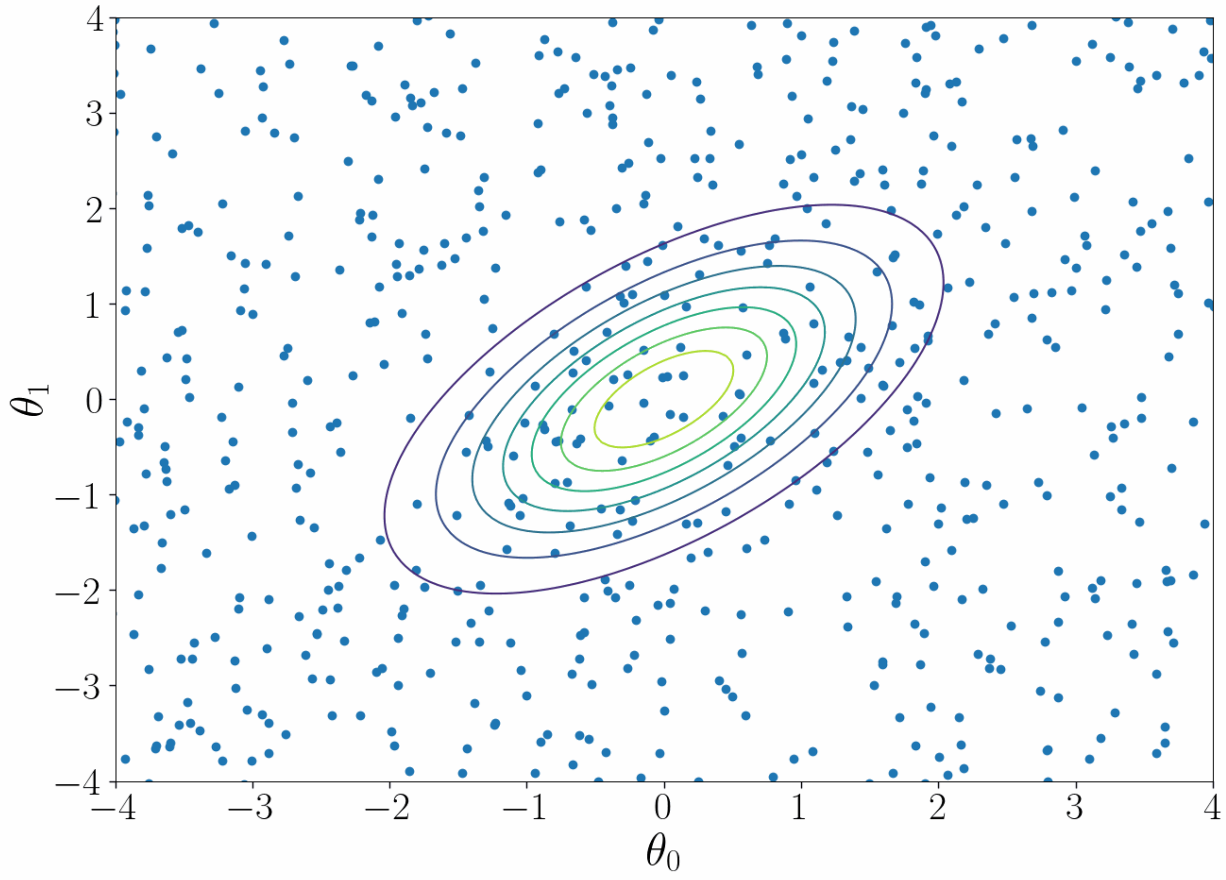

Various open-source samplers

MCMC samplers

- emcee: https://emcee.readthedocs.io/
- ptemcee: https://github.com/willvousden/ptemcee
- PyMC: https://www.pymc.io/
- zeus: https://zeus-mcmc.readthedocs.io/
- ….

Nested samplers

- dynesty: https://dynesty.readthedocs.io/en/latest/
- nessai: https://github.com/mj-will/nessai
- Nestle: http://kylebarbary.com/nestle/
- pymultinest: https://johannesbuchner.github.io/PyMultiNest/index.html
- …

Bilby: a user-friendly Bayesian inference library

- Python codes, installable with pip/conda.
- All the components necessary for CBC parameter inference built in (likelihood, frequently-used priors, useful parameter conversion functions etc.)
- Supports open-source samplers and the native one: bilby-mcmc.
- Can be used for non-CBC problems (See Tutorial 3.1).
- Can simulate CBC signals as well as analyzing real data (See Tutorial 3.2).

Playing with posterior samples

Posterior samples have been released from LVK.

- O1, O2: https://dcc.ligo.org/LIGO-P1800370/public
- O3a: https://zenodo.org/record/6513631
- O3b: https://zenodo.org/record/5546663

In [2]: samples

Out[2]:

	costheta_jn	luminosity_distance_Mpc	right_ascension	declination	m1_detec
0	-0.976633	517.176717	1.456176	-1.257815	
1	-0.700404	401.626864	2.658802	-0.874661	
2	-0.840752	369.579071	1.106548	-1.136396	
3	-0.583657	386.935268	2.077180	-1.246351	
4	-0.928271	345.104345	0.993604	-1.069243	
...	...	...	...	...	
8345	-0.691637	306.985025	1.485646	-1.269228	
8346	-0.834615	462.649414	2.065362	-1.265618	
8347	-0.911463	448.930876	1.536913	-1.257956	
8348	-0.856914	561.020036	2.367289	-1.211824	
8349	-0.919556	519.641782	1.916675	-1.250801	

8350 rows × 10 columns

Playing with posterior samples

In [3]:
```
import matplotlib.pyplot as plt

plt.hist(samples["luminosity_distance_Mpc"], density=True, bins=100)
plt.xlabel("Luminosity distance (Mpc)")
plt.ylabel("Probability distribution")
plt.show()
```

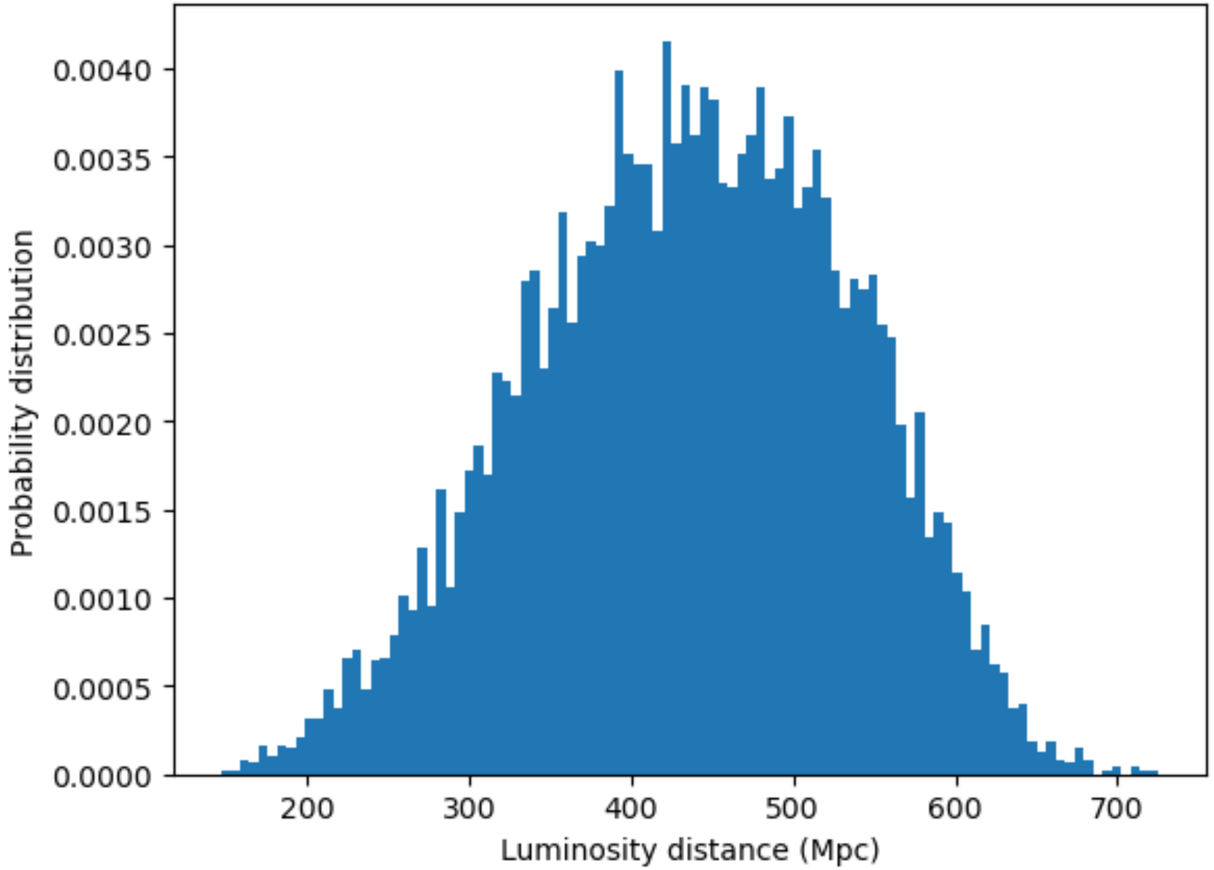

Histogram of samples gives 1D posterior distribution.

The 90% credible interval can be obtained by calculating the 5th and 95th percentiles of samples.

Playing with posterior samples

In [11]:
```
import corner
import numpy as np

corner.corner(
    np.array([samples["right_ascension"], samples["declination"]]).T,
    labels=["RA", "Dec"]
)
```

Out[11]:

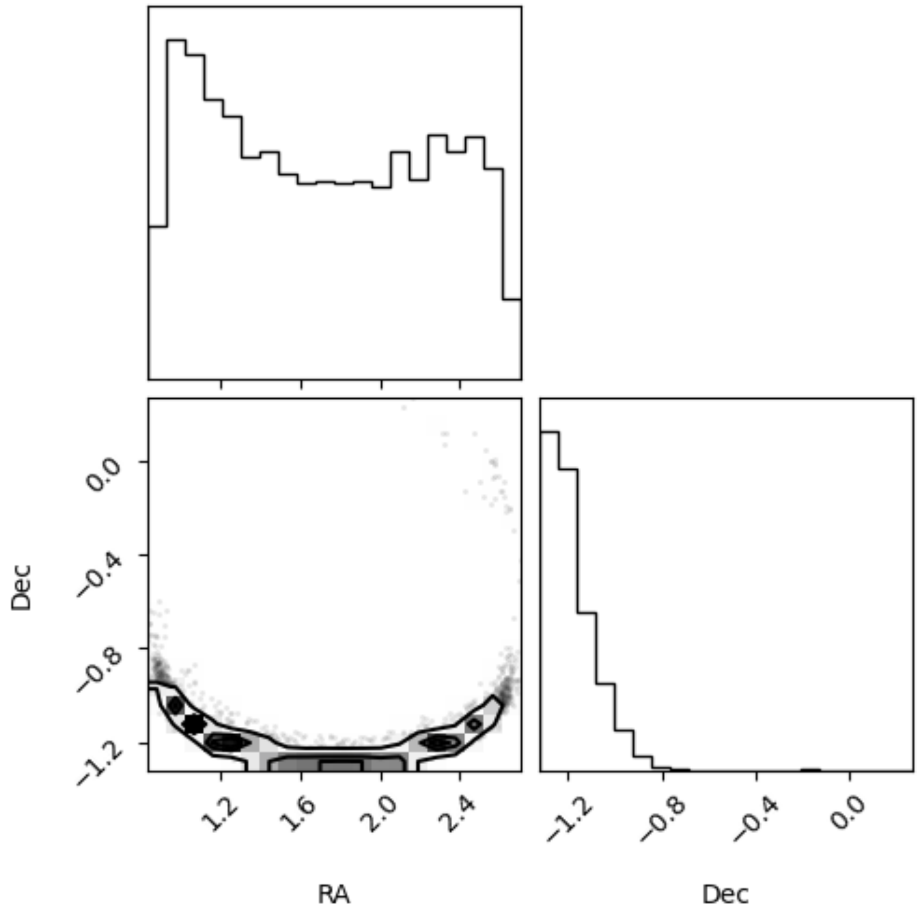

2D histogram is useful to understand parameter correlation.

See Tutorial 3.3 to learn more about reading/plotting samples.

Conclusion

- Source parameters such as masses, spins, and tidal deformabilities of colliding objects can be measured with observed gravitational-wave waveform.
- Source parameter estimation is typically performed with Bayesian inference, where likelihood is computed under the assumption of stationary Gaussian noise.
- We generate random samples following Bayesian posterior probability distribution and make their histograms to estimate source parameter values.
- Useful references
  - Bilby documentation: https://lscsoft.docs.ligo.org/bilby/
  - Thrane and Talbot (2019): https://arxiv.org/abs/1809.02293

Calibration uncertainties

Due to uncertainties in detector calibration, observed signal can be slightly different from true signal:

$$\tilde{h}_{\mathrm{observed}}(f) = \tilde{h}_{\mathrm{true}}(f)\big(1 + \delta A(f)\big)e^{i\delta\phi(f)}.$$

Additional $2N_{\mathrm{nodes}}$ parameters per detector:
$\{\delta A(f_i), \delta\phi(f_i)\} \quad (i = 1,2,\ldots,N_{\mathrm{nodes}})$

L. Sun et al., arXiv: 2107.00129.

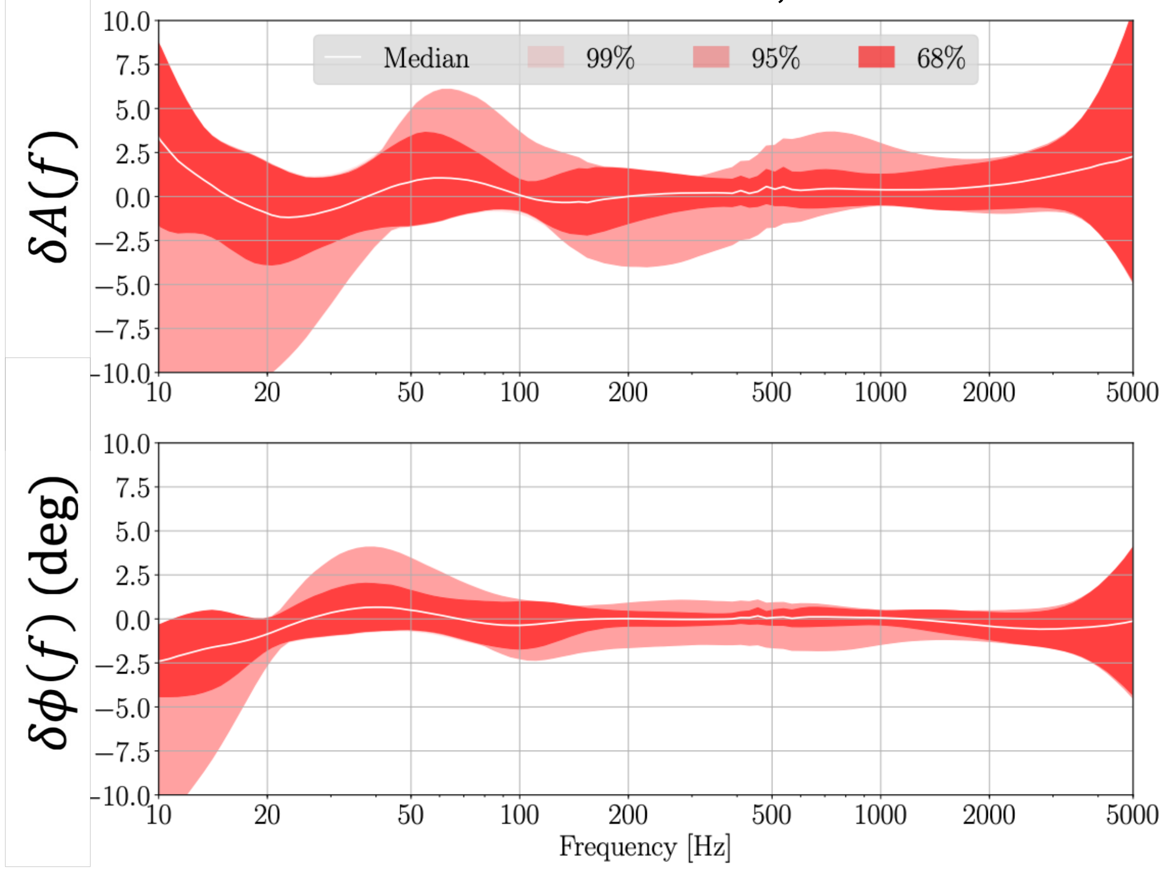

Figure: Calibration uncertainties of amplitude (top) and phase (bottom) of LIGO-Hanford in O3

Tests of general relativity (GR)

Introduce parameters controlling deviation from GR predictions:

$$\tilde{h}(f) = A(f)e^{i\Phi(t)}, \qquad \Phi(t) = \Phi_{GR}(t) + \Delta\varphi_n f^{\frac{n-5}{3}}.$$

Credit: B. P. Abbott et al., PRL **123**, 011102 (2019).

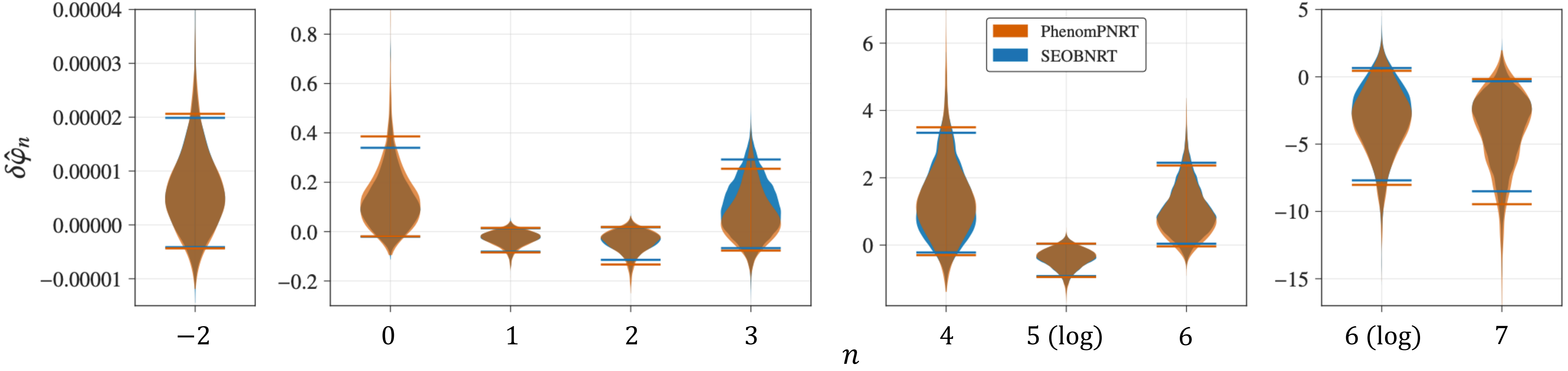

Figure: Constraints on deviation of GW170817 from GR predictions